Spatiotemporal& geostatistical modelling of groundwater level depth over Haryana-Punjab, India

Abstract

The present study focuses on the Haryana and Punjab regions of the Indus basin, India. The study aims to analyze the long-term spatial-temporal changes in the groundwater level from 1996 to 2019. The modelling study involves a twofold objective. First, the ordinary kriging method estimates and evaluates spatial and temporal variations in groundwater level depth (surface-to-water level). Second, the study applies a pixel-based Mann-Kendall trend analysis. The point kriging cross-validation (PKCV) results are optimum, acceptable, and supports the unbiasedness hypothesis of kriging. The trend, significant or not, is determined by the Mann-Kendall test, while Sen's slope estimator determines the slope magnitude of the trend. Results revealed a significantly (at 99% and 95% confidence interval) high-rate depletion zone of groundwater level from 1996–2019 in the southwestern-central region to the western-northern area for all four seasons. The average rate of groundwater level in these zones declined from 40.36 cm/yr. to 37.42 cm/yr. It was observed from trend modelling in the monsoon season for 2014-2019 (Six-year window) that the net per cent area of groundwater level for the study area in the high- and low-rate depletion zone was hiked by 0.90% and 2.17%, respectively.

Keywords: Ordinary kriging, significant trend, Mann-Kendall, Sen's slope.

1 INTRODUCTION

Unveils the long-term spatial-temporal variation of groundwater level and rainfall, provides an effective tool for exploring groundwater depletion zones and is essential for the best management of groundwater resources (Nourani et al., 2008; Rajmohan et al., 2006). *Geostatistics* is the method that provides the kriged map after the optimized model of a semi-variogram with an uncertainty map (kriging variance). Present research work focused on the Haryana and Punjab regions of the Indus Basin, India (Figure 1). The main objective of the present study is to understand the long-term seasonal spatial-temporal behaviour of groundwater level and identify the critical and safe zone with a minimum error factor (Akhtar, S., 2023). Geostatistical methods and pixel-based trend analysis are advanced approaches to understanding groundwater levels (Eastman et al., 2009). Geostatistics delivers several techniques based on the idea of random functions (Uyan & Cay, 2013), which are frequently applied to estimate the value of a spatially measured variable at unknown places (Varouchakis et al., 2019). These techniques are based on the doctrine of the regionalized variables (Uyan & Cay, 2013). A pixel-based spatial analysis of groundwater level observations over time showed where the water level is increasing, decreasing, or has no change. The Mann-Kendall test was used for the significance test, and the associated Sen's slope estimator was used to determine the slope of the trend (Vousoughi et al., 2013). The Haryana and Punjab regions are covered by a vast expanse of quaternary sediments of alluvial and aeolian origin, and the area is covered by hard rocks (Srivastava et al., 2014) in the northeastern part (Tertiary) of the region to the southwestern margin (Archean rock). Because of their favourable geology and over-exploitation of groundwater (Shekhar et al., 2020; Srivastava et al., 2006), landform, and agricultural improvement, the Haryana-Punjab regions have become the leading areas of the country where the livelihood of the inhabitants is primarily dependent on cultivation. If this tendency proceeds and the groundwater management system in this region does not get attention, severe damage will affect the aquifer's surface and subsurface water body(s).

2. DATA AND METHODS

Available data on groundwater level depth (surface-to-water level) exists for all four seasons of Indian cropping patterns (Chowdary et al., 2008; Liu et al., 2021) from 1996 to 2019. These seasons are pre-monsoon (March-May), monsoon (June-September), post-monsoon rabi (September-October) and post-monsoon Kharif (October-December) (http://cgwb.gov.in/wqreports.html). Figure 2 showsthe study's workflow chart.

2.1GEOSTATISTICS

The first methodology is the geostatistics employed was on the groundwater level depth. The semi-variogram is an essential part of geostatistics, and the semi-variogram (ϒ(h)) is estimated as half the average of the quadratic difference between two observations of a variable detached by a distance-vector h. ϒ(h) Semi-variogram function at distance h is defined as:

$$\Upsilon(h) = \frac{1}{2N(h)} \sum_{i=1}^{N(h)} [Z(xi) - Z(xi + h)]^2 \quad \text{---------- (1)}$$

Here in equation (1), N(h) refers to the total number of the variable pairs separated by this distance and Z(xi) indicate the value of the variable. Before developing geostatistical modelling, it is compulsory to evaluate the semi-variogram model, and it is designed for categories of the distance between sample pairs. Semi-variogram modelling work is the most widely used spherical model (Isaaks & Srivastava, 1989). When the nugget variance is not too significant but important with clear range (R) and sill (Co+C, Co-nugget, C-continuity), then a spherical model of semi-variogram is a good selection among other semi-variogram models like Gaussian, exponential etc. (Isaaks & Srivastava, 1989). Cross-validation is a technique used to test the acceptance and adequacy of the developed semi-variogram model. The most appropriate semi-variogram model is chosen on a trial-and-error basis of the point kriging cross-validation (PKCV) technique. This method minimizes the error variance and sets the prediction error's mean to zero so there are no over or underestimates (Giraldo et al., 2011). Kriging is a robust interpolation technique that derives weights from surrounding known values to predict unknown locations. Among the various kriging ways, this part of the present research deals with ordinary kriging for spatial variability analysis of groundwater level depth data from 1996 to 2019. Let G* be the kriged estimate of the mean value of grid G of the samples having values g1, g2,

g3……gn and let a1, a2, a3……an be the weightage giving to each of the values respectively such that Σai=1; and G*=Σaigi. Thus the estimation becomes unbiased; the mean error is zero for a large number of estimated values, and the kriging variance (equation 2) is given as:

$$\sigma_k^2 = \Sigma\,(G_i - G^*)^2 \quad \text{---------- (2)}$$

To construct variance minimum, a coefficient is called Lagrange multiplier (□) (equation 3), used for the optimal solution of the kriging system. To achieve the condition of unbiased estimations of ordinary Kriging, the following set of equations have to be solved concurrently:

$$\begin{cases} \sum_{i=1}^{n} \lambda i \Upsilon(h) - \square = \Upsilon(h) \\ \sum_{i=1}^{n} \lambda i = 1 \end{cases} \quad \text{---------- (3)}$$

Where λi is the weight associated with the data, and the Lagrange multiplier is represented by μ.

2.2 MANN-KENDALL TREND MODELLING

This research's second modelling work employed was a pixel-based Mann-Kendall trend analysis (Fensholt et al., 2009; Eastman et al., 2009) on raster surfaces of kriged groundwater level (After the conversion of kriged groundwater level depth into kriged groundwater level, MSL). The statistical significance of the trend was analyzed using the Mann- Kendall test, and the magnitudes of the trend were estimated using Sen's slope estimator (Sobrino & Julien, 2013). One advantage of this test is that it is not affected by missing data, while another benefit is that the data need not conform to any specific distribution (Jaagus, 2006). Null hypothesis is Ho for Mann-Kendall non-parametric test and alternative hypothesis (H_1) of this test states that the distributions of xk and xj are not identical for all k and j ≤ n with k ≠ j. The Mann–Kendall (M.K.) test statistics denoted by S, having zero mean and a variance estimated by equation (3) is given by;

$$S = \sum_{i=1}^{n-1} \sum_{j=i+1}^{n} \text{sgn}\,(xj - xk) \text{----------(1)}$$

Where xj and xk represent n data points at times j and k respectively, and sgn is the sign function defined by:

$$\text{sgn} = \begin{cases} 1 & \text{if } (xj - xi) > 0 \\ 0 & \text{if } (\text{xj} - \text{xi}) = 0 \\ -1 & \text{if } (\text{xj} - \text{xi}) < 0 \end{cases} \text{----------(2)}$$

For higher values of n, where n>= 10, the M.K. test statistics S follows the approximately normal distribution with mean as zero and variance V(s) as computed by equation (3):

$$\text{V(s)} = \text{n(n} - 1)(2\text{n} + 5) - \sum_{\text{j}=1}^{\text{p}} \text{tj(tj} - 1)(2\text{tj} + 5)/18 \text{ ---------(3)}$$

Where n refers to the number of data points, tj specifies the number of data points in the pth group. Tied groups (a tied group is a set of sample data having the same value) represented are by p. tj is the number of data points in the jth tied groups (Silva et al., 2015). The probability associated with S (equations 1 & 2) and the sample size n were statistically computed to quantify the significance of the trend. Then, the normalized test statistics Zmk computes using equation (4) as given below:

$$Z_{mk} = \begin{cases} \frac{S-1}{\sqrt{\text{var (s)}}}, & \text{when } s > 0 \\ 0, & \text{when } s = 0 \\ \frac{S-1}{\sqrt{\text{var (s)}}}, & \text{when } s < 0 \end{cases} \text{----------(4)}$$

The null hypothesis is rejected at 99% confidence level if p-value ≥ 0.01; similarly, at 95 % confidence level, is rejected if the p-value ≥ 0.05. The resulting trend may have any of the three values (equation 4), i.e., positive, negative or zero (no trend) with a corresponding confidence level.

3. RESULTS AND DISCUSSIONS

Groundwater level depth data were transformed into the log for removing the outliers and good eye visualisation fitting of the semi-variogram model, and after final modelling, all values were back-transformed into original values. Semi-variogram models were cross-validated with the

Point Kriging Cross-Validation Technique (PKCV) and were fitted to the experimental semi-variogram models. Kriging was carried out using the fitted semi-variogram parameters (Figure 3) that led to the generation of prediction and uncertainty(Kriging variance) maps. Parameters of a fitted spherical model of semi-variogram for all four seasons from 1996–2019 are shown in Table 1.(a), Table 1. (b), Table 1.(c) and Table 1.(d). Based on block kriging, kriged estimate (KE) geo-visualization maps for seasonal groundwater level depth with uncertainty are shown in Figure 4 for 1996 and 2019. Block kriging parameters for all four seasons (1996–2019) are shown in Table 2. (a); Table 2. (b); Table 2. (c) & Table 2. (d). Pixel-based trend analysis for spatial-temporal analysis of kriged groundwater level (MSL) employed the non-parametric Mann-Kendall test from 1996-2019. The test was analyzed on kriged estimate raster surfaces of groundwater level (MSL) at 99% and 95% CI. This test was studied in two separate phases for all four seasons' groundwater level (MSL); in the first phase, analyses were conducted from 1996–2019 (Table 3a & Figure 5 a-d); in the second phase, they were performed from 1996–2014 (Table 3b & Figure 5 a-d). Based on these two-phase studies, the entire study area was divided into four zones for the groundwater level. The first zone is a high-rate depletion zone where the range of Sen's slope is -74 cm/yr to -25 cm/yr. The second zone is a low-rate depletion zone where the range of Sen's slope is -26 cm/yr to 0 cm/yr. The third and the fourth zones are slow-rate and fast-rate restoration zones of groundwater levels, respectively. The Sen's slope range for slow-rate restoration is 1–9 cm/yr, while the fast-rate restoration zone is 10–27 cm/yr. It was found from pixel-based MK trend testing of groundwater level (MSL) from 1996 to 2019 that four districts (Kaithal, Karnal, Bathinda, and Barnala) depict very fast-decreasing rates of groundwater levels for all four seasons (Figures 5 a–d). The declination range of groundwater levels in these regions is -74 cm/yr to -54 cm/yr. Besides these four districts, Sangram, Jind, Amritsar, Tarn Taran, Sirsa, Hamirpur, Kapurthala, and Jalandhar districts are within a high-depletion rate zone (Figures 5 a–d). The average Sen's slope (at 99% and 95% CI) in this zone is -37.78 cm/yr in pre-monsoon, -40.78 cm/yr in monsoon, -41.03 cm/yr in post-monsoon (rabi), and -40.12 cm/yr in post-monsoon (Kharif) seasons (Table 3a). It was found from a two-phase(1996–2014 and 1996–2019) time difference window for the years 2014– 2019 in high-rate depletion zones of the net per cent aerial extent of the whole study area significantly increased by 0.90% in monsoon and 0.23% in post-monsoon (rabi) seasons, while in the same zone for pre-monsoon and post-monsoon (Kharif) seasons, net per cent areas significantly shrank up to 3.57%

and 0.47%, respectively (Table 3 (c); Figure 6a and 6b). Further, this study found that in the low-rate depletion zone of groundwater level (MSL), a large net per cent aerial extent of the whole study area was gained by 5.89% in pre-monsoon, 2.17% in monsoon, 5.28% in post-monsoon (rabi), and 5.48% post-monsoon (Kharif) seasons (Table 3 (c); Figure 6a and 6b). These results indicate that the monsoon and post-monsoon (rabi) season is critical for places in the high-rate depletion zone. However, these areas showed positive results in pre-monsoon and post-monsoon (Kharif) seasons concerning the area with a high groundwater level depletion rate. Results also revealed that places in the low-rate depletion zone of groundwater level (MSL) are critical for all four seasons regarding the significantly increasing net per cent area rate in this zone (2014–2019, time range difference of two phase time window). In high-rate restoration zones, the net per cent aerial extent of groundwater level from 2014–2019 was estimated at -0.22% in pre-monsoon, 9.82% in monsoon, -0.97% in post-monsoon (rabi) and -0.83% in post-monsoon (Kharif) seasons (Table 3 (c); Figure 6a and 6b). These results revealed that the districts of Faridabad, Fazlika, Bhiwani, and Muktasar are safe in monsoon seasons regarding the high-rate restoration zone of groundwater level (MSL) because the area is significantly increasing in this zone.

4 CONCLUSIONS

The present research work was conducted in two steps. The first step of the modelling work was the geostatistical modelling of groundwater level depth. From the kriged variance maps (uncertainty), it was observed that dark grey showed a minimum error, and light colour indicated a maximum error (Figure 4). It was also observed from these maps for all four seasons (Figure 4) that the error is less wherever dug wells are present, and it gradually increases as the location moves farther away from the dug wells. Based on uncertainty (Kriging variance maps), results revealed that new dug wells construction is needed from the eastern-central region to the northern region of the study area. Pixel-based trend results revealed a significant (at 99% and 95% CI) high- and low-rate depletion zone of groundwater level in the southwestern-central to the western-northern regions for all four seasons from 1996 to 2019. These areas are critical, and groundwater levels continuously decrease with time. Districts in these zones are Sangram, Jind, Amritsar, Tarn Taran, Sirsa, Hamirpur, Kapurthala, Jalandhar, Kaithal, Karnal, Bathinda, and Barnala. Results also revealed that most parts of the periphery regions of the study areas are safe in the monsoon seasons regarding the fast-rate restoration zone of groundwater level because the

net per cent area is significantly increasing in this zone. The main cultivated cropping seasons are monsoon and post-monsoon (rabi); in these two seasons, groundwater levels continuously decrease from 1996 to 2019, and the area of depletion zone of groundwater level is also spreading. These adverse results were obtained due to overexploitation of groundwater for irrigation purposes.

References

Akhtar, S. (2023). Spatial-temporal Trends Mapping and Geostatistical Modelling of Groundwater Level Depth Over Northern Parts of Indo-Gangetic Basin, India. *Journal of Geography, Environment and Earth Science International*, *27*(10), 96–112. https://doi.org/10.9734/jgeesi/2023/v27i10719

Central Groundwater Bored. Retrieved September 15, 2021, from http://cgwb.gov.in/wqreports.html

Chowdary, V. M., Chandran, R. V., Neeti, N., Bothale, R. V, Srivastava, Y. K., Ingle, P., Ramakrishnan, D., Dutta, D., Jeyaram, A., Sharma, J. R., & Singh, R. (2008). Assessment of surface and sub-surface waterlogged areas in irrigation command areas of Bihar state using remote sensing and GIS. *Agricultural Water Management*, *95*(7), 754–766. https://doi.org/10.1016/j.agwat.2008.02.009

da Silva, R. M., Santos, C. A. G., Moreira, M., Corte-Real, J., Silva, V. C. L., & Medeiros, I. C. (2015). Rainfall and river flow trends using Mann–Kendall and Sen's slope estimator statistical tests in the Cobres River basin. *Natural Hazards*, *77*(2), 1205–1221. https://doi.org/10.1007/s11069-015-1644-7

Fensholt, R., Rasmussen, K., Nielsen, T. T., & Mbow, C. (2009a). Evaluation of earth observation based long term vegetation trends - Intercomparing NDVI time series trend analysis consistency of Sahel from AVHRR GIMMS, Terra MODIS and SPOT VGT data. *Remote Sensing of Environment*, *113*(9), 1886–1898. https://doi.org/10.1016/j.rse.2009.04.004

Fensholt, R., Rasmussen, K., Nielsen, T. T., & Mbow, C. (2009b). Evaluation of earth observation based long term vegetation trends - Intercomparing NDVI time series trend analysis consistency of Sahel from AVHRR GIMMS, Terra MODIS and SPOT VGT data. *Remote Sensing of Environment*, *113*(9), 1886–1898. https://doi.org/10.1016/j.rse.2009.04.004

Giraldo, R., Delicado, P., & Mateu, J. (2011). Ordinary kriging for function-valued spatial data. *Environmental and Ecological Statistics*, *18*(3), 411–426. https://doi.org/10.1007/s10651-010-0143-y

Jaagus, J. (2006). Climatic changes in Estonia during the second half of the 20th century in relationship with changes in large-scale atmospheric circulation. *Theoretical and Applied*

Climatology, *83*(1–4), 77–88. https://doi.org/10.1007/s00704-005-0161-0

Liu, T., Mickley, L. J., Gautam, R., Singh, M. K., DeFries, R. S., & Marlier, M. E. (2021). Detection of delay in post-monsoon agricultural burning across Punjab, India: Potential drivers and consequences for air quality. *Environmental Research Letters*, *16*(1). https://doi.org/10.1088/1748-9326/abcc28

Neeti, N., & Eastman, J. R. (2011). A Contextual Mann-Kendall Approach for the Assessment of Trend Significance in Image Time Series. *Transactions in GIS*, *15*(5), 599–611. https://doi.org/10.1111/j.1467-9671.2011.01280.x

Nourani, V., Mogaddam, A. A., & Nadiri, A. O. (2008). An ANN-based model for spatiotemporal groundwater level forecasting. *Hydrological Processes*, *22*(26), 5054–5066. https://doi.org/10.1002/hyp.7129

Rajmohan, N., & Elango, L. (2006). Hydrogeochemistry and its relation to groundwater level fluctuation in the Palar and Cheyyar river basins, southern India. *Hydrological Processes*, *20*(11), 2415–2427. https://doi.org/10.1002/hyp.6052

Shekhar, S., Kumar, S., Densmore, A. L., van Dijk, W. M., Sinha, R., Kumar, M., Joshi, S. K., Rai, S. P., & Kumar, D. (2020). Modelling water levels of northwestern India in response to improved irrigation use efficiency. *Scientific Reports*, *10*(1), 1–16. https://doi.org/10.1038/s41598-020-70416-0

Sobrino, J. A., & Julien, Y. (2013). Trend analysis of global MODIS-terra vegetation indices and land surface temperature between 2000 and 2011. *IEEE Journal of Selected Topics in Applied Earth Observations and Remote Sensing*, *6*(5), 2139–2145. https://doi.org/10.1109/JSTARS.2013.2239607

Srivastava, G. S., S1ngh, I. B., & Kulshrestha, A. K. (2006). LATE QUATERNARY GEOMORPHIC EVOLUTION OF YAMUNA-SUTLEJ INTERFLUVE: SIGNIFICANCE OF TERMINAL FAN. In *Journal of the Indian Society of Remote Sensing* (Vol. 34, Issue 2).

Srivastava, G. S., Singh, I. B., & Kulshrestha, A. K. (2014). Geomorphic and tectonic features of Punjab-Haryana plain as identified from digital elevation model and surface profiles. *Himalayan Geology*, *35*(2), 97–109.

Uyan, M., & Cay, T. (2013). Spatial analyses of groundwater level differences using geostatistical modeling. *Environmental and Ecological Statistics*, *20*(4), 633–646. https://doi.org/10.1007/s10651-013-0238-3

Varouchakis, E. A., Theodoridou, P. G., & Karatzas, G. P. (2019). Spatiotemporal geostatistical modeling of groundwater levels under a Bayesian framework using means of physical background. *Journal of Hydrology*, *575*, 487–498. https://doi.org/10.1016/j.jhydrol.2019.05.055

Vousoughi, F. D., Dinpashoh, Y., Aalami, M. T., & Jhajharia, D. (2013). Trend analysis of groundwater using non-parametric methods (case study: Ardabil plain). *Stochastic*

Environmental Research and Risk Assessment, *27*(2), 547–559. https://doi.org/10.1007/s00477-012-0599-4

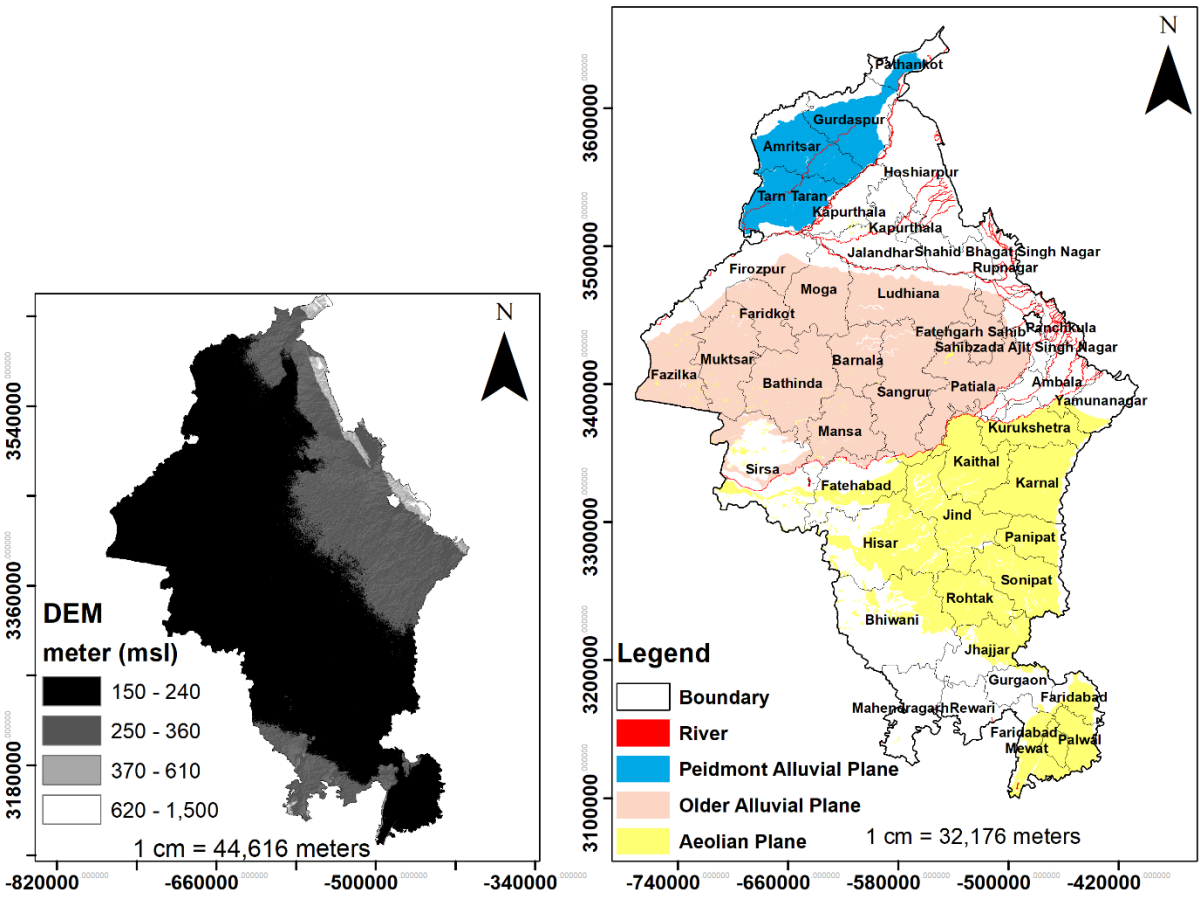

Figure 1. Study area.

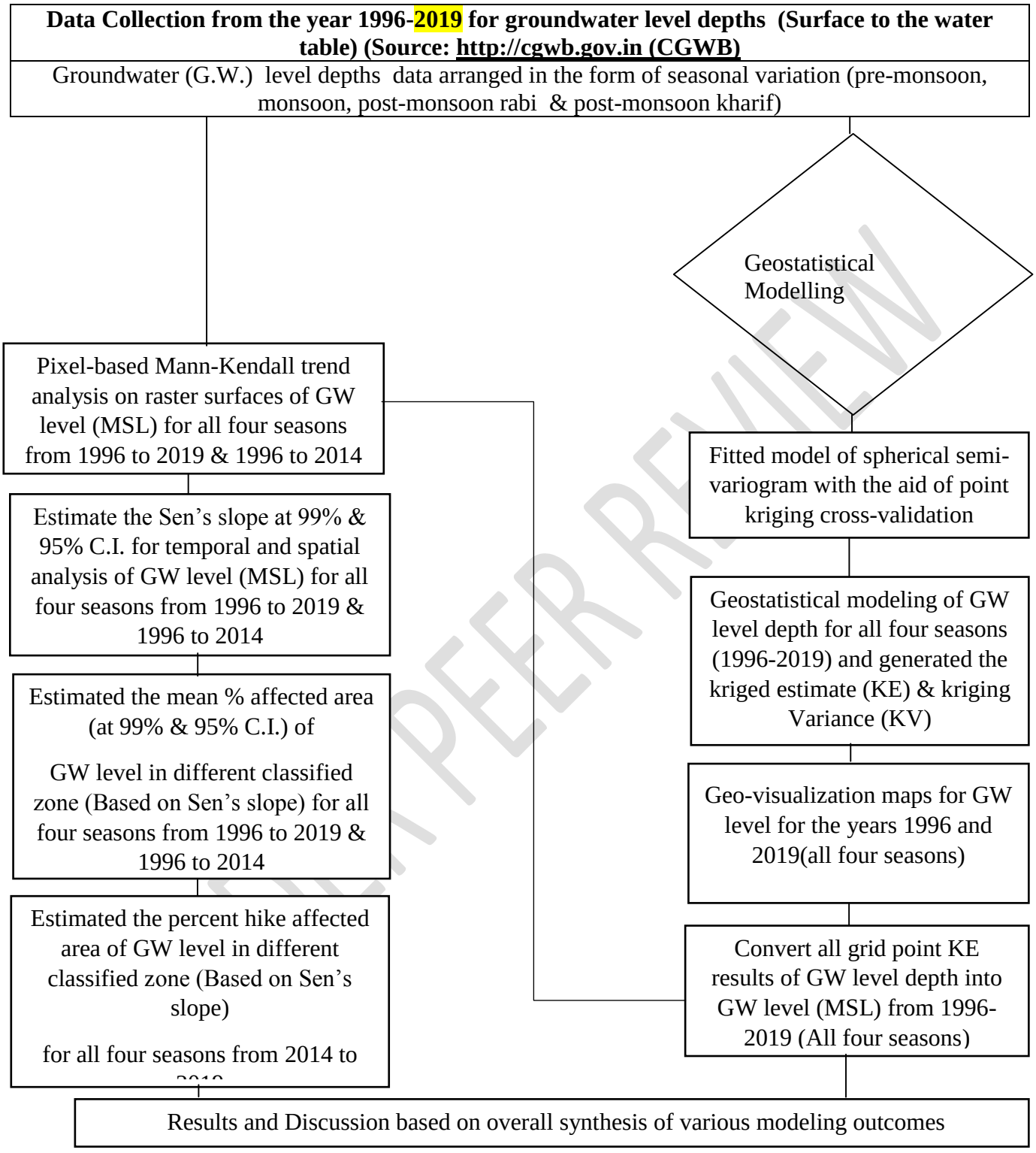

Figure 2 Workflow diagram of the research work

Table 1(a). Point kriging cross-validation parameters for spherical model semi-variogram of pre-monsoon season from years 1996 to 2019.

Year	Co m^2	C m^2	Sill (C+Co) m^2	Range (m)	Mean (Z-Z*) (m)	% Error due to parameters	Mean KE log (m)	EV:KV
1996	0.020	0.053	0.0730	54926.00	0.001	0.18	0.8100	1.03
1997	0.028	0.037	0.0650	70333.22	0.002	0.29	0.7901	0.99
1998	0.038	0.043	0.0810	66730.00	0.001	0.21	0.7700	0.95
1999	0.030	0.040	0.0700	65370.00	0.002	0.36	0.7500	1.02
2000	0.036	0.032	0.0680	70372.26	0.002	0.29	0.8100	0.97
2001	0.024	0.036	0.0600	72136.68	0.002	0.28	0.8100	0.99
2002	0.024	0.042	0.0660	69355.70	0.002	0.26	0.8100	1.05
2003	0.031	0.031	0.0620	74778.87	0.002	0.26	0.8600	0.98
2004	0.035	0.040	0.0750	66105.40	0.002	0.32	0.8250	0.97
2005	0.025	0.040	0.0650	64852.42	0.002	0.26	0.8260	1.01
2006	0.038	0.050	0.0880	81945.71	0.004	0.50	0.8000	1.01
2007	0.037	0.061	0.0980	78792.32	0.003	0.44	0.7800	1.05
2008	0.030	0.060	0.0900	88517.00	0.002	0.28	0.8500	0.96
2009	0.034	0.060	0.0940	100348.00	0.004	0.53	0.8200	0.99
2010	0.025	0.070	0.0950	74244.00	0.004	0.52	0.8400	0.99
2011	0.030	0.080	0.1100	68506.24	0.003	0.45	0.7900	1.05
2014	0.011	0.092	0.1030	70141.00	0.007	0.90	0.8200	1.05
2015	0.029	0.042	0.0710	69653.82	0.008	1.09	0.7900	1.05
2017	0.015	0.075	0.0900	50000.00	0.008	0.99	0.8000	0.98
2018	0.040	0.12	0.1600	83238.62	0.001	0.45	1.0304	1.04
2019	0.030	0.11	0.1400	88464.00	0.008	0.08	1.0065	1.05

Table 1(b). Point kriging cross-validation parameters for spherical model semi-variogram of monsoon season from years 1996 to 2019

Year	Co m^2	C m^2	Sill (C+Co) m^2	Range (m)	Mean (Z-Z*) (m)	% Error due to parameters	Mean KE log (m)	EV:KV
1996	0.08	0.07	0.150	81028.41	0.0010	0.13	0.7530	1.05
1997	0.05	0.03	0.080	80751.58	0.0006	0.08	0.7500	0.95
1998	0.05	0.04	0.090	69501.52	0.0001	0.13	0.7551	0.95
1999	0.04	0.05	0.090	55829.36	0.0012	0.16	0.7652	0.95
2000	0.05	0.03	0.080	56171.30	0.0016	0.21	0.7650	0.95
2001	0.04	0.05	0.090	71278.00	0.0016	0.22	0.7550	0.96
2002	0.03	0.04	0.070	75207.98	0.0014	0.16	0.8300	1.05
2003	0.05	0.04	0.090	63722.14	0.0026	0.32	0.8200	0.96
2004	0.05	0.03	0.080	76077.00	0.0061	0.74	0.8200	0.95
2005	0.04	0.05	0.090	62111.22	0.0004	0.04	0.8100	0.96
2006	0.04	0.05	0.090	85439.32	0.0033	0.42	0.8001	1.03
2007	0.08	0.08	0.160	91828.02	0.0024	0.31	0.7560	1.05
2008	0.04	0.09	0.130	92336.89	0.0011	0.14	0.8000	0.96
2009	0.04	0.06	0.100	100546.8	0.0055	0.67	0.8100	0.95
2010	0.03	0.08	0.110	79423.80	0.0024	0.29	0.8200	1.05
2011	0.09	0.09	0.180	91004.20	0.0076	1.06	0.7100	0.95
2014	0.01	0.11	0.120	71508.50	0.0094	1.12	0.8302	1.03
2015	0.05	0.06	0.110	83685.00	0.0029	0.38	0.7500	1.05
2017	0.02	0.10	0.120	50000.00	0.0036	0.47	0.7505	1.01
2018	0.04	0.13	0.170	90632.94	0.0010	0.23	1.0258	1.02
2019	0.06	0.14	0.200	90450.93	0.0020	0.20	0.9652	1.05

Table 1(c). Point kriging cross-validation parameters for spherical model semi-variogram of post-monsoon (rabi) season from years 1996 to 2019

Year	Co m^2	C m^2	Sill (C+Co) m^2	Range (m)	Mean (Z-Z*) (m)	% Error due to parameters	Mean KE log (m)	EV:KV
1996	0.03	0.06	0.090	55214.97	0.001	0.22	0.7664	0.98
1997	0.04	0.04	0.080	77457.51	0.001	0.16	0.7540	0.95
1998	0.05	0.05	0.100	61299.00	0.001	0.26	0.7350	0.95
1999	0.05	0.05	0.100	57994.00	0.027	0.39	0.6810	0.95
2000	0.05	0.03	0.080	82444.50	0.029	0.38	0.7513	0.95
2001	0.03	0.04	0.070	70759.83	0.002	0.33	0.7498	0.98
2002	0.02	0.05	0.070	73388.04	0.001	0.15	0.7698	1.01
2003	0.04	0.04	0.080	78169.0	0.002	0.25	0.8280	1.02
2004	0.04	0.05	0.090	65029.00	0.002	0.25	0.7936	0.95
2005	0.03	0.04	0.070	62971.00	0.002	0.26	0.8038	0.98
2006	0.05	0.06	0.110	80006.00	0.003	0.41	0.7792	0.95
2007	0.04	0.06	0.100	84774.76	0.003	0.38	0.7879	1.01
2008	0.03	0.08	0.110	85646.96	0.002	0.34	0.8124	0.98
2009	0.04	0.08	0.120	94000.21	0.004	0.60	0.7776	0.98
2010	0.04	0.08	0.120	89124.00	0.005	0.69	0.7869	0.95
2011	0.05	0.09	0.140	79015.00	0.003	0.47	0.7568	0.95
2014	0.01	0.10	0.110	81076.00	0.009	1.22	0.8020	1.02
2015	0.03	0.06	0.090	53000.00	0.005	0.78	0.7543	1.05
2017	0.02	0.08	0.100	81766.53	0.008	1.03	0.8083	1.03
2018	0.05	0.13	0.180	88819.24	0.001	0.24	0.9887	1.05
2019	0.04	0.14	0.180	72157.63	0.001	0.37	0.9821	1.02

Table 1(d). Point kriging cross-validation parameters for spherical model semi-variogram of post-monsoon (kharif) season from years 1996 to 2019.

Year	Co m^2	C m^2	Sill (C+Co) m^2	Range (m)	Mean (Z-Z*) (m)	% Error due to parameters	Mean KE log (m)	EV:KV
1996	0.03	0.09	0.120	50076.32	0.009	0.12	0.7301	1.04
1997	0.05	0.05	0.100	64550.61	0.001	0.17	0.7451	0.95
1998	0.07	0.45	0.520	64772.58	0.001	0.16	0.7000	0.95
1999	0.04	0.04	0.080	59551.68	0.001	0.24	0.7453	0.96
2000	0.04	0.04	0.080	78864.15	0.001	0.20	0.7751	0.95
2001	0.03	0.04	0.070	71201.55	0.002	0.28	0.7750	0.98
2002	0.03	0.04	0.070	78074.00	0.002	0.32	0.8200	1.01
2003	0.05	0.05	0.100	63011.45	0.002	0.35	0.7801	0.97
2004	0.05	0.04	0.090	71171.15	0.002	0.98	0.8200	0.98
2005	0.03	0.07	0.100	62691.00	0.002	0.02	0.7751	0.99
2006	0.04	0.06	0.100	76444.26	0.002	0.30	0.7752	0.99
2007	0.04	0.06	0.100	92567.18	0.002	0.37	0.7753	0.98
2008	0.03	0.09	0.120	93605.87	0.002	0.30	0.7751	0.97
2009	0.04	0.08	0.120	98130.83	0.004	0.54	0.7754	0.96
2010	0.04	0.09	0.130	89124.78	0.005	0.64	0.7751	0.99
2011	0.05	0.08	0.130	84720.90	0.003	0.51	0.7451	0.95
2014	0.01	0.11	0.120	77970.47	0.007	0.90	0.8200	1.03
2015	0.04	0.06	0.100	76330.44	0.008	1.05	0.7551	1.05
2017	0.04	0.08	0.120	55504.68	0.008	1.07	0.7650	0.95
2018	0.04	0.13	0.170	90911.83	0.001	0.93	0.9906	1.05
2019	0.04	0.15	0.190	69132.68	0.001	0.85	0.9719	1.03

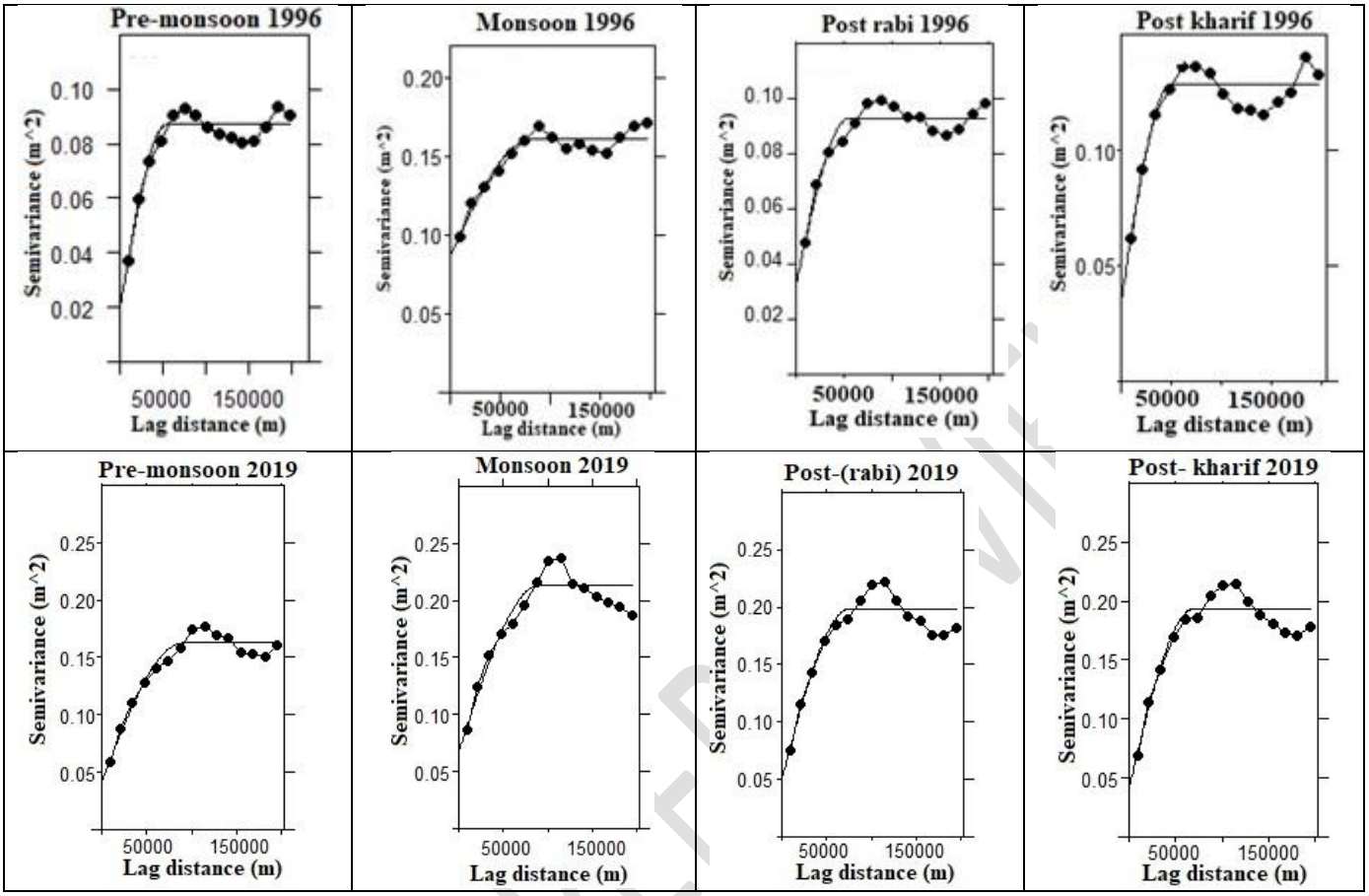

Figure 2. fitted spherical model of semi-variogram for all four seasons for the years 1996, and 2019.

Table 2(a). Geostatistical Parameters for pre-monsoon season's groundwater level depth (Surface to the water table) from the year 1996 to 2019.

Year	Mean kriged estimate (Log value)	Kriged estimate (K.E.) after the backlog transformation of mean log of K.E. (meter)	Mean kriged estimate (K.E.) from MSL	Mean kriging variance (K.V.)
1996	0.8394	6.91	231.16	0.023
1997	0.8450	7.00	231.07	0.013
1998	0.8102	6.46	231.61	0.016
1999	0.7937	6.22	231.85	0.014
2000	0.8692	7.14	230.93	0.012
2001	0.8579	7.21	230.86	0.016
2002	0.8796	7.58	230.49	0.017
2003	0.9169	8.26	229.81	0.025
2004	0.9068	8.07	230.00	0.018
2005	0.9063	8.06	230.01	0.019
2006	0.9063	8.06	230.01	0.020
2007	0.8549	7.16	230.91	0.026
2008	0.9380	8.67	229.40	0.023
2009	0.9429	8.77	229.30	0.020
2010	0.9518	8.95	229.12	0.028
2011	0.8976	7.90	230.17	0.030
2014	0.9201	8.32	229.75	0.023
2015	0.8432	6.97	231.10	0.031
2017	0.9014	7.97	230.10	0.060
2018	1.0643	11.59	226.48	0.021
2019	1.0578	11.42	226.65	0.030

Table 2(b).Geostatistical Parameters for monsoon season's groundwater level depth (Surface to the water table) fror 1996 to 2019.

Year	Mean kriged estimate (Log value) (meter)	Kriged estimate (K.E.) after the backlog transformation of mean log of K.E. (meter)	Mean kriged estimate (K.E.) from MSL (meter)	Mean kriging variance (K.V.) (meter)
1996	0.7534	5.66	232.41	0.010
1997	0.7639	5.80	232.27	0.013
1998	0.7663	5.84	232.23	0.020
1999	0.7844	6.08	231.99	0.020
2000	0.7930	5.41	232.66	0.008
2001	0.7845	6.08	231.99	0.020
2002	0.8746	7.49	230.58	0.016
2003	0.8653	7.33	230.74	0.008
2004	0.8823	7.62	230.45	0.016
2005	0.8576	7.20	230.87	0.025
2006	0.8683	7.38	230.69	0.022
2007	0.7933	6.21	231.86	0.002
2008	0.8445	6.99	231.08	0.008
2009	0.8939	7.83	230.24	0.023
2010	0.8764	7.52	230.55	0.032
2011	0.7982	6.28	231.79	0.042
2014	0.8635	7.30	230.77	0.054
2015	0.8277	6.72	231.35	0.031
2017	0.8181	6.57	231.50	0.071
2018	1.0405	10.10	227.97	0.016
2019	1.0436	11.05	227.02	0.014

Table 2 (c). Geostatistical Parameters for post-monsoon (rabi) season's groundwater level depth (Surface to the water table) from the year 1996 to 2019.

Year	Mean kriged estimate (Log value)	Kriged estimate (K.E.) after the backlog transformation of mean log of K.E. (meter)	Mean kriged estimate (K.E.) from MSL	Mean kriging variance (K.V.)
1996	0.7668	5.85	232.22	0.008
1997	0.7753	5.96	232.11	0.014
1998	0.7426	5.53	232.54	0.009
1999	0.7010	5.02	233.05	0.022
2000	0.7767	5.98	232.09	0.012
2001	0.7772	5.99	232.08	0.015
2002	0.8154	6.54	231.53	0.018
2003	0.8614	7.27	230.80	0.014
2004	0.8450	7.00	231.07	0.022
2005	0.8515	7.10	230.97	0.020
2006	0.8537	7.14	230.93	0.023
2007	0.8408	6.93	231.14	0.023.
2008	0.8714	7.44	230.63	0.030
2009	0.8563	7.18	230.89	0.027
2010	0.8587	7.22	230.85	0.031
2011	0.8214	6.63	231.44	0.009
2014	0.8350	6.84	231.23	0.053
2015	0.8136	6.51	231.56	0.043
2017	0.8695	7.40	230.67	0.042
2018	1.0027	10.06	228.01	0.042
2019	1.0413	11.00	227.07	0.041

Table 2(d). Geostatistical Parameters for post-monsoon (kharif) season's groundwater level depth (Surface to the water table) from the year 1996 to 2019.

Year	Mean kriged estimate (Log value)	Kriged estimate (K.E.) after the backlog transformation of mean log of K.E. (meter)	Mean kriged estimate (K.E.) from MSL	Mean kriging variance (K.V.)
1996	0.7224	5.28	232.79	0.036
1997	0.7588	5.74	232.33	0.019
1998	0.7150	5.19	232.88	0.021
1999	0.7681	5.86	232.21	0.017
2000	0.8065	6.40	231.67	0.013
2001	0.8031	6.35	231.72	0.016
2002	0.8649	7.33	230.74	0.016
2003	0.8382	6.89	231.18	0.025
2004	0.8769	7.53	230.54	0.019
2005	0.8761	7.52	230.55	0.019
2006	0.8426	6.96	231.11	0.024
2007	0.8412	6.94	231.13	0.025
2008	0.8544	7.15	230.92	0.033
2009	0.8674	7.37	230.70	0.028
2010	0.8567	7.19	230.88	0.034
2011	0.8182	6.58	231.49	0.035
2014	0.8714	7.44	230.63	0.057
2015	0.8092	6.44	231.63	0.037
2017	0.8365	6.86	231.21	0.043
2018	1.0105	10.24	227.83	0.037
2019	1.0420	11.02	227.05	0.042

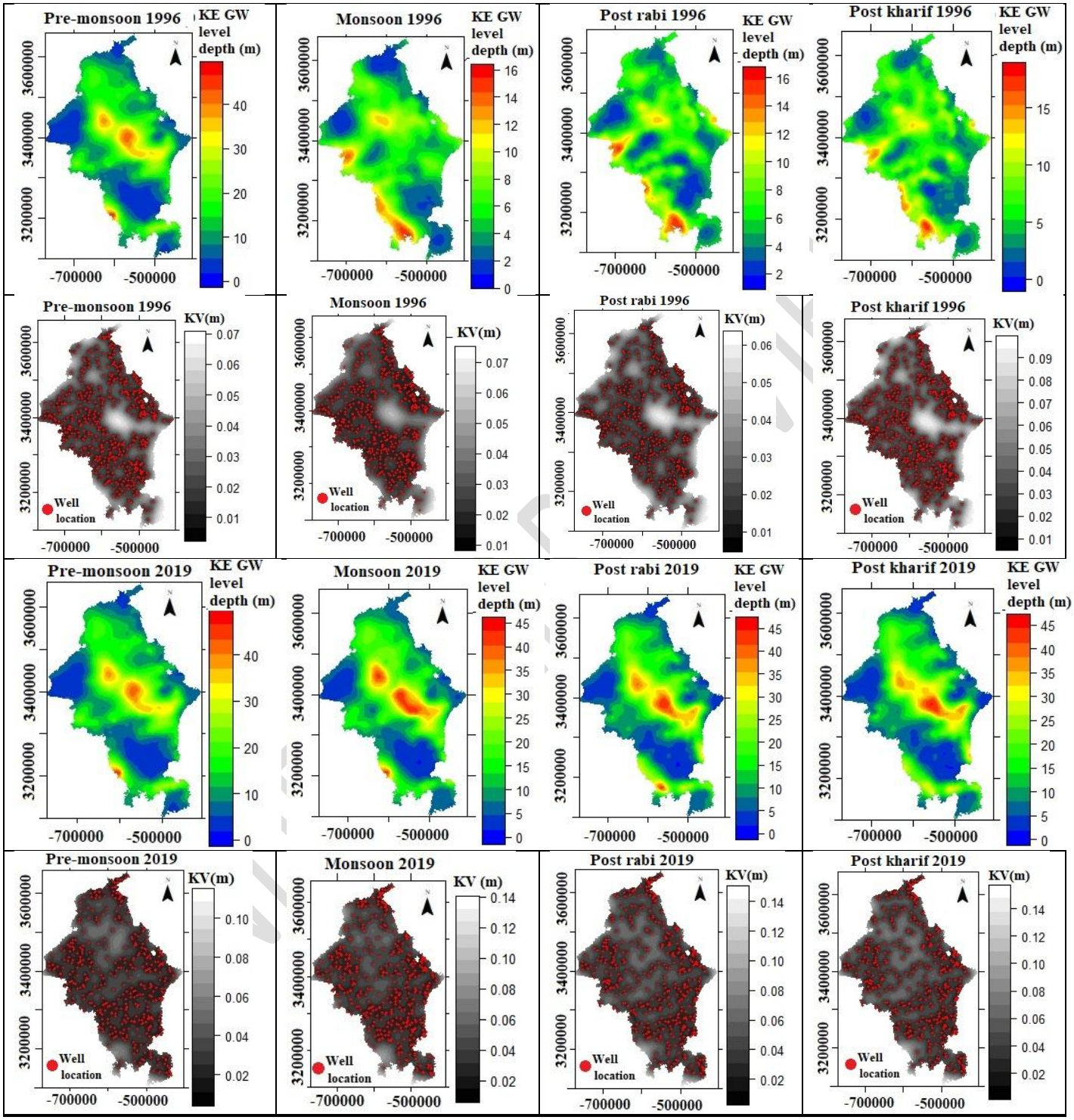

Figure (3). Geo-visualization kriged maps with kriging variance (uncertainty) (1996 and 2019) for all four seasons

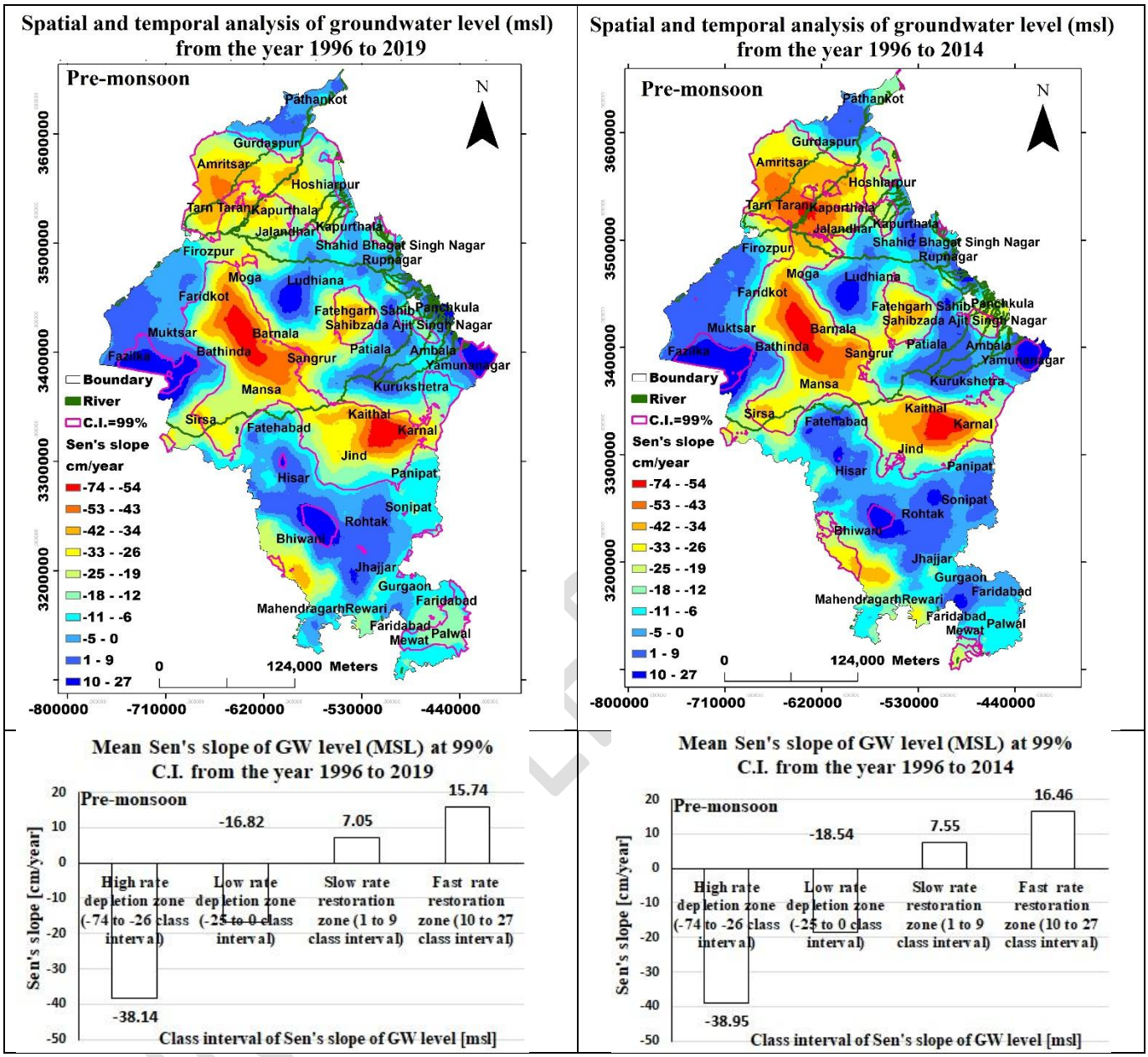

Figure 5(a). Spatial and temporal analysis of groundwater level (MSL) and Sen's slope for pre-monsoon season from the years 1996 to 2019 and 1996 to 2014.

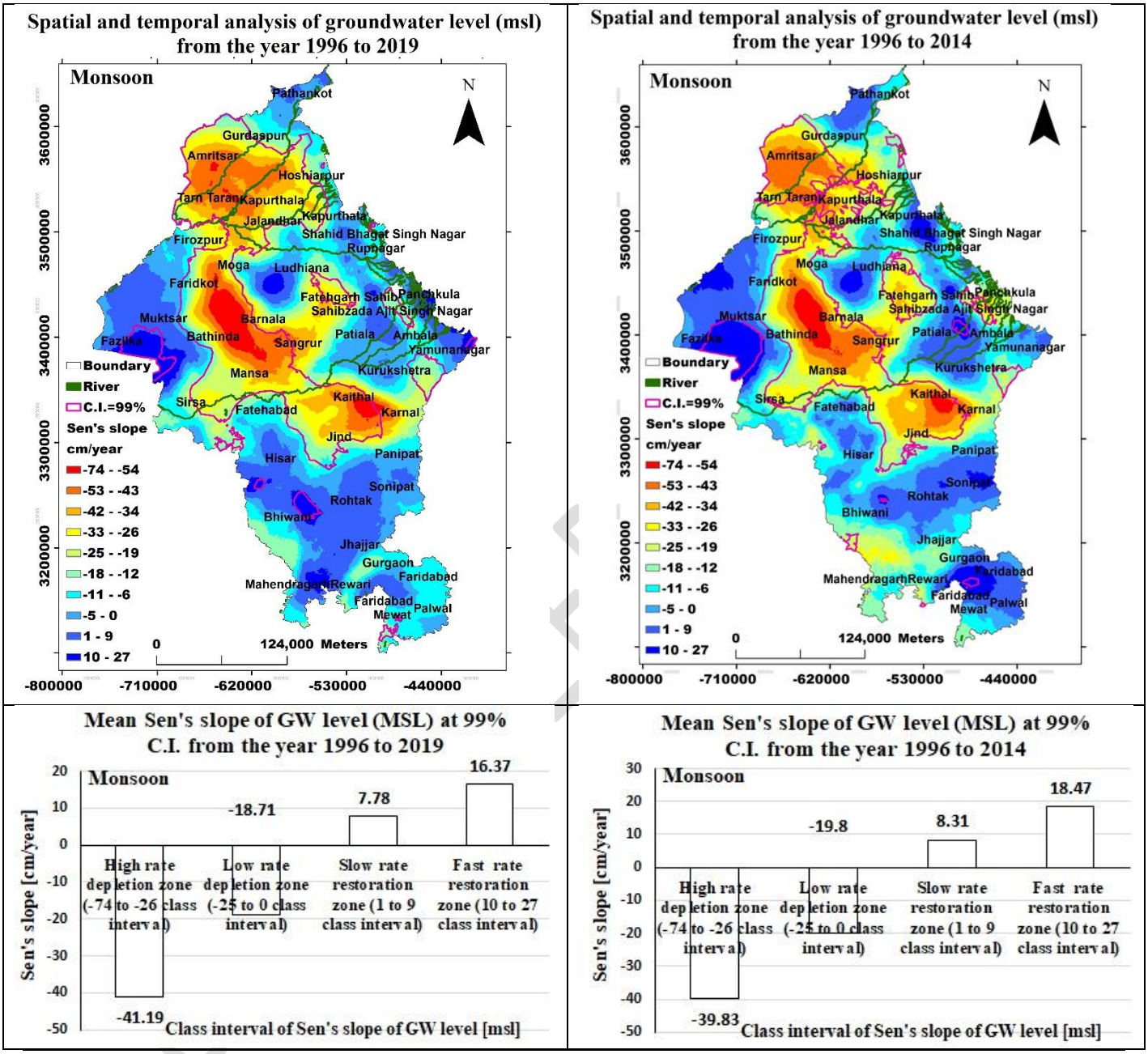

Figure 5(b). Spatial and temporal analysis of groundwater level (MSL) and Sen's slope for the monsoon season from the years 1996 to 2019 and 1996 to 2014

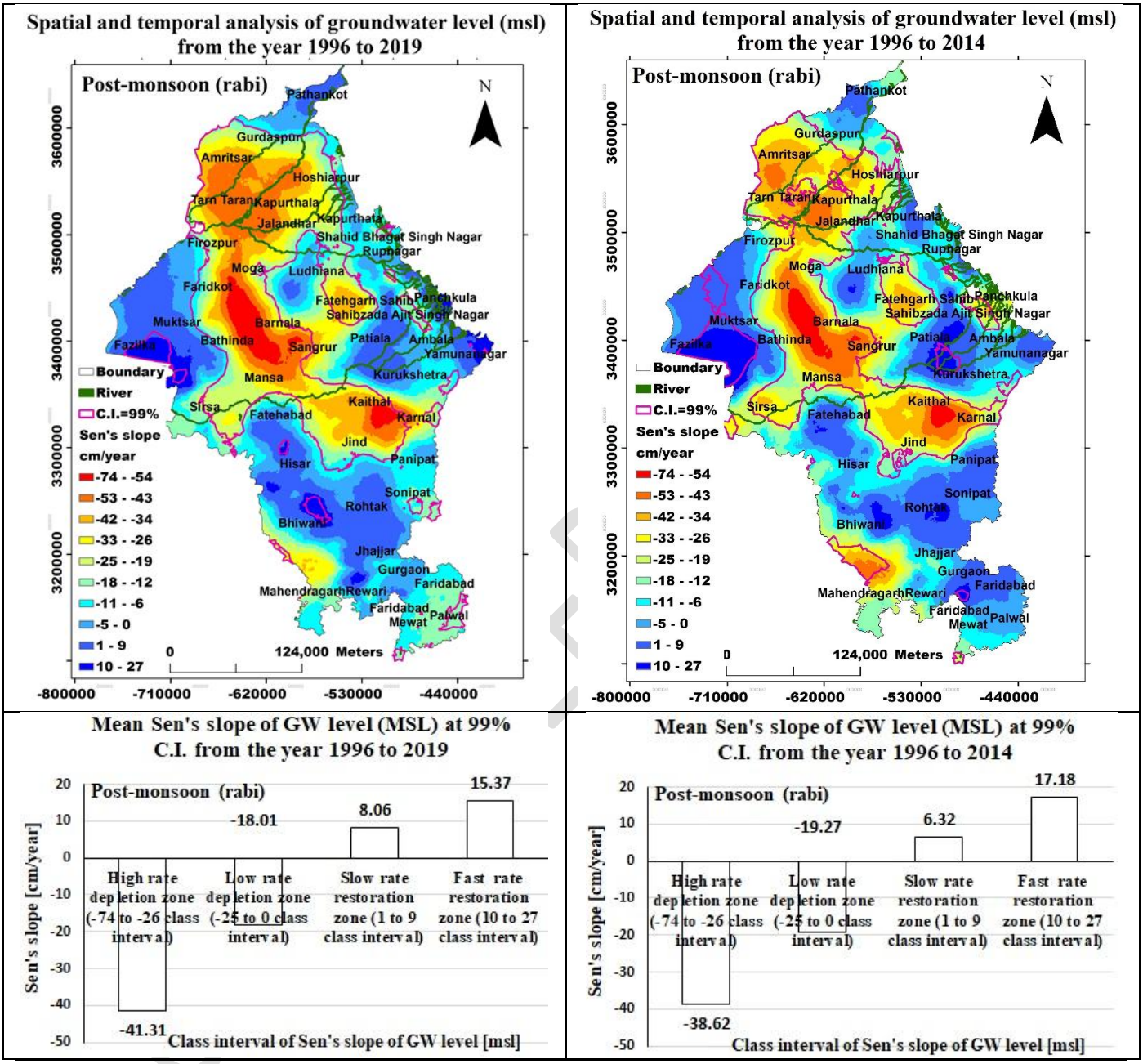

Figure 5(c). Spatial and temporal analysis of groundwater level (MSL) and Sen's slope for post-monsoon (rabi) season from the years 1996 to 2019 and 1996 to 2014

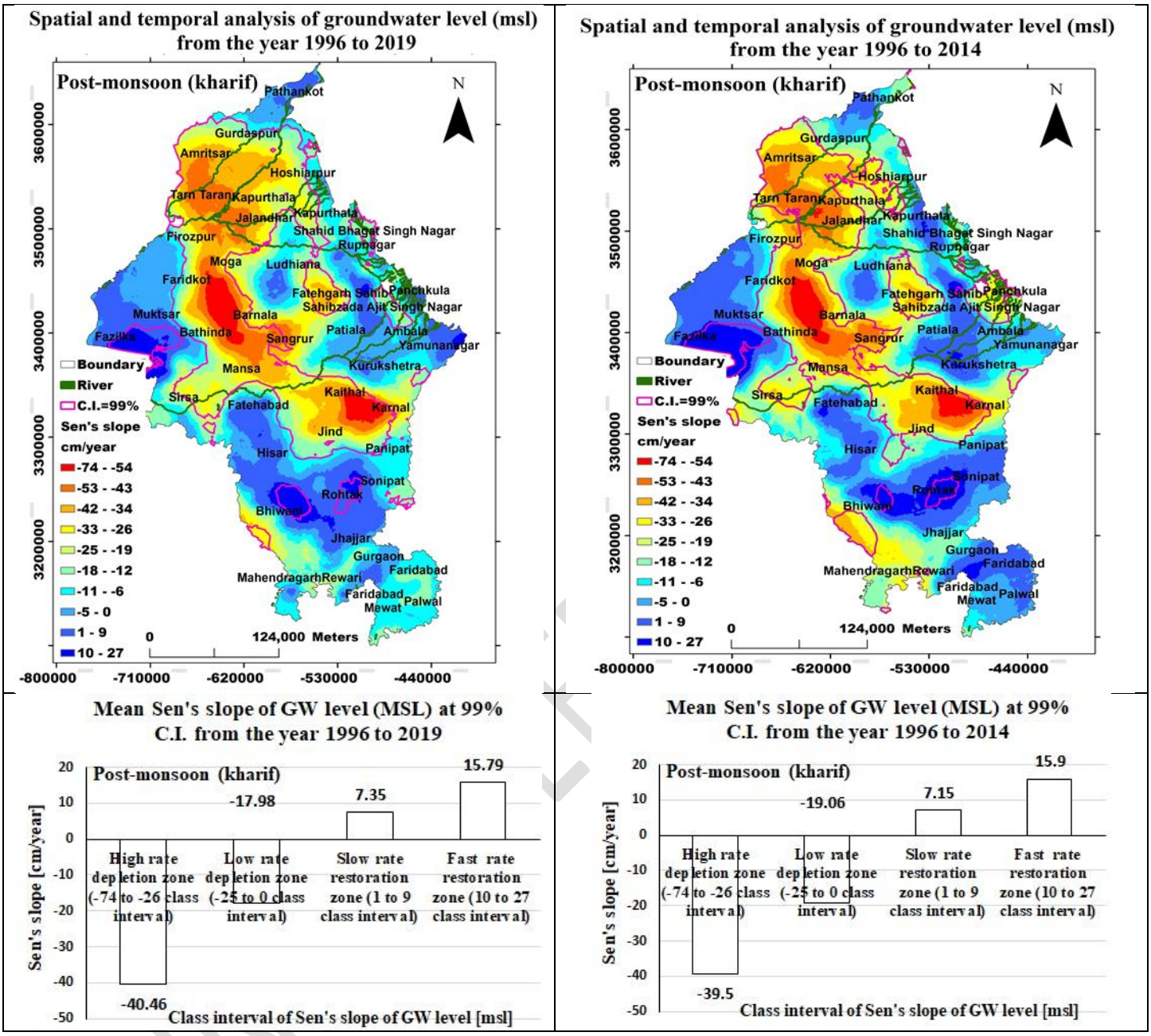

Figure 5(d).Spatial and temporal analysis of groundwater level (MSL) and Sen's slope for post-monsoon (kharif) season from the years 1996 to 2019 and 1996 to 2014.

Table 3(a). Sen's slope magnitude and percent affected area of groundwater level (MSL) in the significant region of the selected class interval from the year 1996 to 2019

(A) Average Sen's slope and per cent affected area of groundwater level (MSL) at 99 % and 95% C.I. in high rate depletion zone (-74 to -26 class interval of Sen's slope)									
Seasons	**P value range**		**Area (Km^2)**			**Mean Sen's slope (cm/year)**		**Affected percent area (Km^2)**	
	99% C.I.	**95% C.I.**	**99% C.I.**	**95% C.I.**	**Total area**	**99% C.I.**	**95% C.I.**	**99% C.I.**	**95% C.I.**
Pre-monsoon	0 to 0.009	0 to 0.048	17817.87	21333.71	96918.41	-38.14	-37.42	18.38	22.01
Monsoon	0 to 0.009	0 to 0.049	20211.26	23467.83	96918.41	-41.19	-40.36	20.85	24.21
Post-monsoon (rabi)	0 to 0.009	0 to 0.049	23820.00	25741.95	96918.41	-41.31	-40.75	24.58	26.56
Post-monsoon (kharif)	0 to 0.009	0 to 0.048	22836.74	25381.00	96918.41	-40.46	-39.78	23.56	26.19
(B) Average Sen's slope and percent affected area of groundwater level (MSL) at 99 % and 95% C.I. in low rate depletion zone (-25 to -0 class interval of Sen's slope)									
Pre-monsoon	0 to 0.009	0 to 0.048	13702.04	25014.57	96918.41	-16.82	-15.55	14.14	25.81
Monsoon	0 to 0.009	0 to 0.048	7120.61	15897.31	96918.41	-18.71	-16.68	7.35	16.40
Post-monsoon (rabi)	0 to 0.009	0 to 0.048	11834.35	21961.77	96918.41	-18.01	-15.82	12.21	22.66
Post-monsoon (kharif)	0 to 0.008	0 to 0.049	10615.54	20000.50	96918.41	-17.98	-16.19	10.95	20.64
(C) Average Sen's slope and percent affected area of groundwater level (MSL) at 99 % and 95% C.I. in low rate restoration zone (1 to 9 class interval of Sen's slope)									
Pre-monsoon	0 to 0.009	0 to 0.048	519.29	1513.63	96918.41	7.05	6.62	0.54	1.56
Monsoon	0 to 0.009	0 to 0.049	122.48	891.75	96918.41	7.78	6.98	0.13	0.92
Post-monsoon (rabi)	0 to 0.009	0 to 0.049	96.28	861.61	96918.41	8.06	7.32	0.10	0.89
Post-monsoon (kharif)	0 to 0.009	0 to 0.049	721.49	2187.40	96918.41	7.35	7.08	0.74	2.26
(D) Average Sen's slope and percent affected area of groundwater level (MSL) at 99 % and 95% C.I. in high rate restoration zone (10 to 27 class interval of Sen's slope)									
Pre-monsoon	0 to 0.009	0 to 0.048	2201.19	2418.35	96918.41	15.74	15.62	2.27	2.50
Monsoon	0 to 0.009	0 to 0.049	7120.61	15897.31	96918.41	16.37	15.45	7.35	16.40
Post-monsoon (rabi)	0 to 0.009	0 to 0.049	1083.73	1958.73	96918.41	15.37	14.63	1.12	2.02
Post-monsoon (kharif)	0 to 0.009	0 to 0.049	1507.34	2007.95	96918.41	15.79	15.24	1.56	2.07

Table 3(b).Sen's slope magnitude and percent affected area of groundwater level (MSL) in the significant region of the selected class interval from the year 1996 to 2014

(A) Average Sen's slope and per cent affected area of groundwater level (MSL) at 99 % and 95% C.I. in high rate depletion zone (-74 to -26 class interval of Sen's slope)									
Seasons	**P value range**		**Area (Km^2)**			**Mean Sen's slope (cm/year)**		**Affected percent area**	
	99% C.I.	**95% C.I.**	**99% C.I.**	**95% C.I.**	**Total area**	**99% C.I.**	**95% C.I.**	**99% C.I.**	**95% C.I.**
Pre-monsoon	0 to 0.009	0 to 0.048	21909.64	24160.64	96918.41	-38.95	-38.31	22.61	24.93
Monsoon	0 to 0.009	0 to 0.043	18930.92	22992.62	96918.41	-39.83	-38.76	19.53	23.72
Post-monsoon (rabi)	0 to 0.009	0 to 0.043	23187.69	25922.21	96918.41	-38.62	-37.94	23.92	26.75
Post-monsoon (kharif)	0 to 0.009	0 to 0.048	22557.19	26578.74	96918.41	-39.50	-38.41	23.27	27.42
(B) Average Sen's slope and percent affected area of groundwater level (MSL) at 99 % and 95% C.I. in low rate depletion zone (-25 to -0 class interval of Sen's slope)									
Pre-monsoon	0 to 0.08	0 to 0.043	9242.78	18068.96	96918.41	-18.54	-17.01	9.54	18.64
Monsoon	0 to 0.009	0 to 0.043	5363.73	13451.26	96918.41	-19.80	-18.09	5.53	13.88
Post-monsoon (rabi)	0 to 0.08	0 to 0.043	7628.02	15932.73	96918.41	-19.27	-17.42	7.87	16.44
Post-monsoon (kharif)	0 to 0.009	0 to 0.043	5700.66	14295.42	96918.41	-19.06	-17.94	5.88	14.75
(C) Average Sen's slope and percent affected area of groundwater level (MSL) at 99 % and 95% C.I. in low rate restoration zone (1 to 9 class interval of Sen's slope)									
Pre-monsoon	0 to 0.08	0 to 0.043	140.22	1191.83	96918.41	7.55	6.47	0.14	1.23
Monsoon	0 to 0.009	0 to 0.043	73.77	537.55	96918.41	8.31	7.47	0.08	0.55
Post-monsoon (rabi)	0 to 0.08	0 to 0.043	893.78	2378.47	96918.41	6.32	6.13	0.92	2.45
Post-monsoon (kharif)	0 to 0.009	0 to 0.043	197.57	598.42	96918.41	7.15	6.84	0.20	0.62
(D) Average Sen's slope and percent affected area of groundwater level (MSL) at 99 % and 95% C.I. in high rate restoration zone (10 to 27 class interval of Sen's slope)									
Pre-monsoon	0 to 0.009	0 to 0.043	2189.67	2854.73	96918.41	16.46	16.11	2.26	2.95
Monsoon	0 to 0.009	0 to 0.043	1593.12	2399.74	96918.41	18.47	17.17	1.64	2.48
Post-monsoon (rabi)	0 to 0.009	0 to 0.043	2189.26	2727.33	96918.41	17.18	16.11	2.26	2.81
Post-monsoon (kharif)	0 to 0.009	0 to 0.043	2101.43	3036.80	96918.41	15.90	15.05	2.17	3.13

Table 3(c)Net percent affected area in a defined class interval of Sen's slope from the year 2014 to 2019 and average % affected area, Sen's slope (at 99% & (%% C.I.) from the years 1996 to 2014 and 1996 to 2019.

(A) Average Sen's slope, per cent affected area of groundwater level (MSL) at 99 % and 95% C.I. and net % area in high rate depletion zone (-74 to -26 class interval of Sen's slope)					
Seasons	**Average affected % area**	**Average Sen's slope**	**Average affected % area**	**Average Sen's slope**	**Net percent affected area**
	1996 to 2014 (years)		**1996 to 2019 (years)**		**2014 to 2019 years**
Pre-monsoon	23.77	-38.63	20.20	-37.78	-3.57
Monsoon	21.63	-39.30	22.53	-40.78	0.90
Post-monsoon (rabi)	25.34	-38.28	25.57	-41.03	0.23
Post-monsoon (kharif)	25.35	-38.96	24.88	-40.12	-0.47
(B) Average Sen's slope, percent affected area of groundwater level (MSL) at 99 % and 95% C.I. and net % area in low rate depletion zone (-25 to -0 class interval of Sen's slope)					
Pre-monsoon	14.09	-17.78	19.98	-16.19	5.89
Monsoon	9.71	-18.95	11.88	-17.70	2.17
Post-monsoon (rabi)	12.16	-18.35	17.44	-16.92	5.28
Post-monsoon (kharif)	10.32	-18.50	15.80	-17.09	5.48
(C) Average Sen's slope, percent affected area of groundwater level (MSL) at 99 % and 95% C.I. and net % area in low rate restoration zone (1 to 9 class interval of Sen's slope)					
Pre-monsoon	0.69	7.01	1.05	6.84	0.36
Monsoon	0.32	7.89	0.53	7.38	0.21
Post-monsoon (rabi)	1.69	6.23	0.50	7.69	-1.19
Post-monsoon (kharif)	0.41	7.00	1.50	7.22	1.09
(D) Average Sen's slope, percent affected area of groundwater level (MSL) at 99 % and 95% C.I. and net % area in high rate restoration zone (10 to 27 class interval of Sen's slope)					
Pre-monsoon	2.61	16.29	2.39	15.68	-0.22
Monsoon	2.06	17.82	11.88	15.91	9.82
Post-monsoon (rabi)	2.54	16.65	1.57	15.00	-0.97
Post-monsoon (kharif)	2.65	15.48	1.82	15.52	-0.83

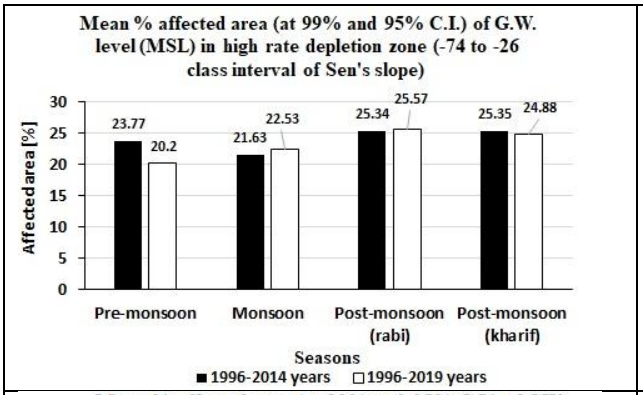

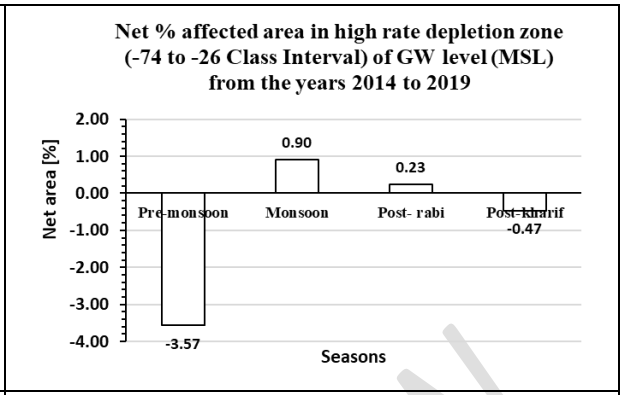

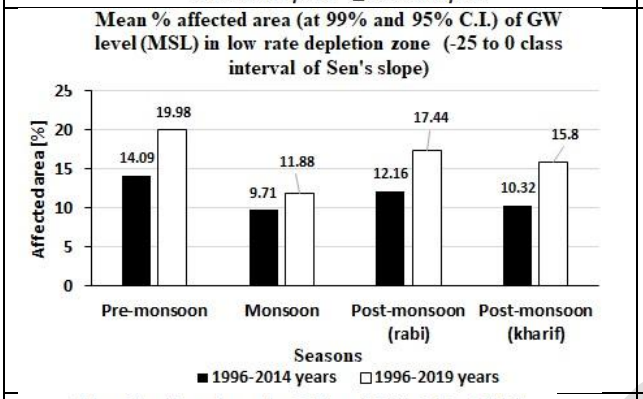

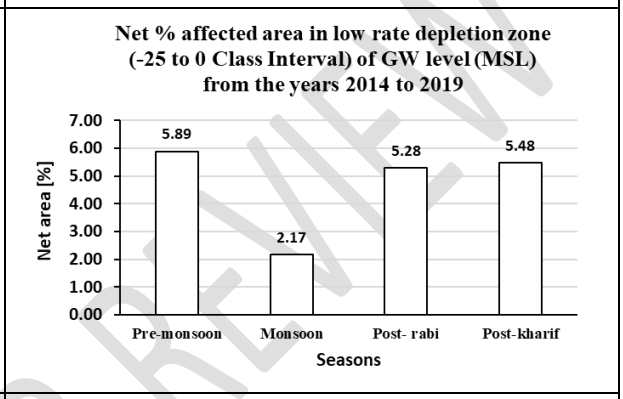

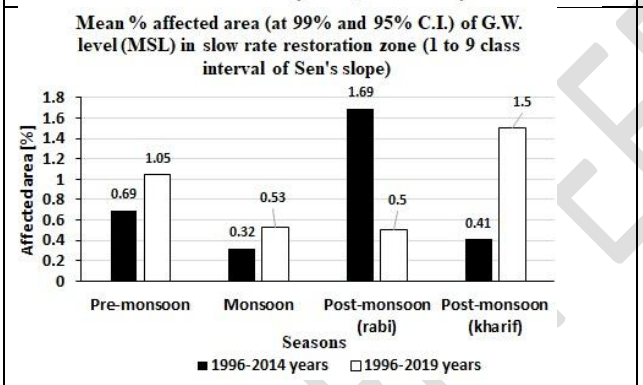

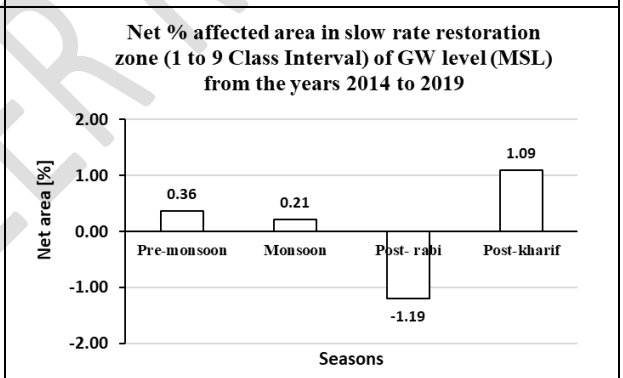

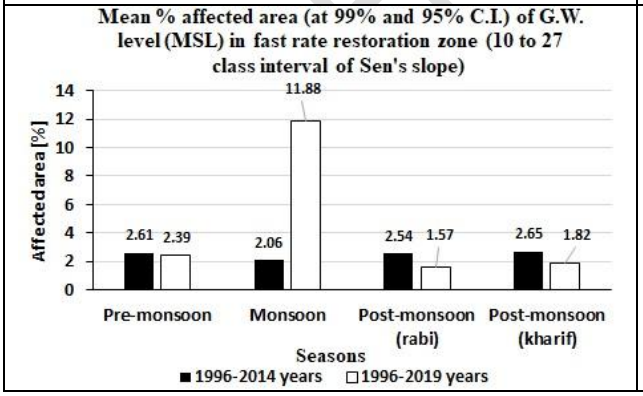

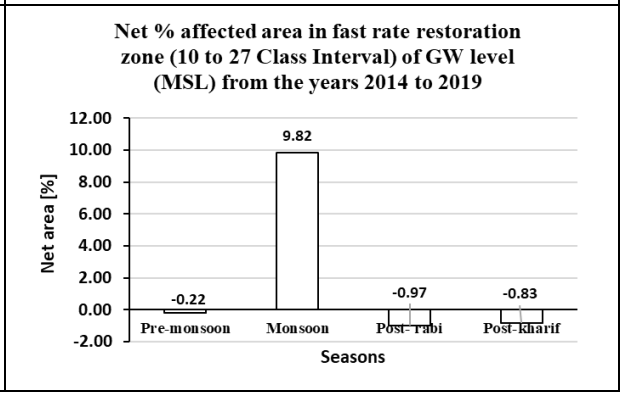

Figure 6(a). Mean percent affected area (at 99% and 95% Confidence Interval) from the years 1996 to 2019 and 1996 to 2014.

Figure 6(b). Net percent affected area from the year 2014 to 2019.